

Table 1 Known structure types of ternary II-III₂ (III-III')-Ch₄ or quaternary II-II'(I₂)-IV-CH₄ (II = Mg, Ca, Sr, Ba, Eu and Yb; II' = divalent transition metal; I = Li, Na, Cu and Ag; III = B, Al, Ga and In; III' = Yb, Sb and Bi; IV = Ge and Sn; Ch = S, Se and Te) compounds. All these data are from ICSD or Pearson's crystal data^a

Compound	Space group	Crystal system	Pearson code	Phase prototype
MgAl ₂ S ₄	<i>Pnma</i>	Orthorhombic	<i>oP28</i>	Mg ₂ SiO ₄
MgAl ₂ S ₄	<i>R3m</i>	Trigonal	<i>hR7</i>	ZnIn ₂ S ₄
MgAl ₂ S ₄	<i>R3̄m</i>	Trigonal	<i>hR7</i>	ZnIn ₂ S ₄
MgGa ₂ S ₄	<i>C2/c</i>	Monoclinic	<i>mS84</i>	MgGa ₂ S ₄
MgIn ₂ S ₄	<i>Fd3̄m</i>	Cubic	<i>cF56</i>	MgAl ₂ O ₄
MgIn ₂ Te ₄	<i>I42m</i>	Tetragonal	<i>tI14</i>	Cu ₂ HgI ₄
SrB ₂ S ₄	<i>P2₁/c</i>	Monoclinic	<i>mP28</i>	SrB ₂ S ₄
SrB ₂ S ₄	<i>R3</i>	Trigonal	<i>hR63</i>	SrB ₂ S ₄
SrAl ₂ S ₄	<i>Cccm</i>	Orthorhombic	<i>oS28</i>	BaGe ₂ Se ₄
SrAl ₂ S ₄	<i>Fddd</i>	Orthorhombic	<i>oF224</i>	EuGa ₂ S ₄
SrGa ₂ Te ₄	<i>I4/mcm</i>	Tetragonal	<i>tI14</i>	CaIn ₂ Te ₄
SrCu ₂ GeSe ₄	<i>Ama2</i>	Orthorhombic	<i>oS32</i>	SrCu ₂ GeSe ₄
SrCu ₂ SnS ₄	<i>P3₁</i>	Trigonal	<i>hP24</i>	SrCu ₂ SnS ₄
SrCu ₂ SnS ₄	<i>P3₂21</i>	Trigonal	<i>hP24</i>	SrCu ₂ SnS ₄
BaB ₂ S ₄	<i>Cc</i>	Monoclinic	<i>mS28</i>	BaB ₂ S ₄
BaAl ₂ S ₄	<i>Pa3̄</i>	Cubic	<i>cP84</i>	BaAl ₂ S ₄
BaAl ₂ Se ₄	<i>P4/nnc</i>	Tetragonal	<i>tP28</i>	BaAl ₂ Se ₄
BaAl ₂ Te ₄	<i>P4/nbm</i>	Tetragonal	<i>tP14</i>	BaAl ₂ Te ₄
BaSbBS ₄	<i>Pnma</i>	Orthorhombic	<i>oP28</i>	KBaPO ₄
BaBiBS ₄	<i>C2/m</i>	Monoclinic	<i>mS28</i>	BaBiBS ₄
BaAg ₂ GeS ₄	<i>I42m</i>	Tetragonal	<i>tI16</i>	K ₃ VO ₄
BaAg ₂ SnS ₄	<i>I222</i>	Orthorhombic	<i>oI16</i>	BaAg ₂ SnS ₄
BaAu ₂ SnS ₄	<i>P2₁2₁2</i>	Orthorhombic	<i>oP32</i>	BaAu ₂ SnS ₄
BaCdSnS ₄	<i>Fdd</i>	Orthorhombic	<i>oF224</i>	BaCdSnS ₄
BaHgSnS ₄	<i>Pnn2</i>	Orthorhombic	<i>oP28</i>	BaHgSnS ₄
EuNa ₂ SiSe ₄	<i>R3c</i>	Trigonal	<i>hR48</i>	EuNa ₂ SiSe ₄
EuNa ₂ GeSe ₄	<i>I43m</i>	Cubic	<i>cI16</i>	Tl ₃ VS ₄
YbCaInS ₄	<i>Pnma</i>	Orthorhombic	<i>oP28</i>	Mg ₂ SiO ₄

^a As there are so many members can be classified to this family, only one compound was chosen as a representative for each type of structure. All these data are checked results from Inorganic Crystal Structure Data (ICSD) and Pearson's Crystal Data (PCD).

obtained by solid-state reactions with KI as flux. The starting materials are stoichiometric mixture of Eu₂O₃, Zn, Ge and S for 1, Eu₂O₃, Ga₂O₃ and S for 2, Eu₂O₃, In₂O₃ and S for 3, and Eu₂O₃, In₂O₃ and Se for 4. A certain amount of boron powder and KI were added to each sample as reducing reagent and flux, respectively. Each sample has a total mass of 500 mg and 400 mg KI additional. The mixtures of starting materials were ground into fine powder in an agate mortar and pressed into pellets, followed by being loaded into quartz tubes. The tubes were evacuated to be 1×10^{-4} torr and flame-sealed. The samples were placed into a muffle furnace, heated from room temperature to 573 K in 5 h and equilibrated for 10 h, followed by heating to 923 K in 5 h and equilibrated for another 10 h, then heated to 1223 K in 5 h and homogenized for 10 days, finally cooled down to 573 K in 5 days and powered off. All the crystals of 1–4 stable in moisture and air were obtained and hand-picked under a microscope since the yields were not high, then washed using ethanol and water under ultrasonic wave, whose purities were confirmed by powder X-ray diffraction (PXRD) study. The PXRD patterns were collected with a Bruker

D8 Advance diffractometer at 40 kV and 100 mA for CuK α radiation ($\lambda = 1.5406 \text{ \AA}$) with a scan speed of 5° min^{-1} at room temperature. The simulated patterns were produced using Mercury v2.3 program provided by the Cambridge Crystallographic Data Center and single-crystal reflection data. A representative PXRD pattern of 3 corresponds well with the simulated one (Fig. 1), indicating it is phase-pure of the selected crystals. Semiquantitative microscope element analysis on the as-prepared single crystals was performed on a field-emission scanning electron microscope (FESEM, HITACHI S-4800II) equipped with an energy dispersive X-ray spectroscopy (EDS, Bruker, Quantax), which confirmed the presence of each elements with the approximate compositions of 1–4. The exact compositions were established from X-ray structure determination.

Structure determination. The intensity data set was collected on Bruker D8 QUEST X-ray diffractometer with graphite-monochromated MoK α radiation ($\lambda = 0.71073 \text{ \AA}$). The structures were solved by direct methods and refined by full-matrix least-squares techniques on F^2 with anisotropic thermal parameters for all atoms. All the calculations were performed with Siemens Shelxtl-97 crystallographic software package.¹⁶ The final refinement included anisotropic displacement parameters for all atoms and a secondary extinction correction. The crystallographic data, atomic coordinates and equivalent isotropic displacement parameter, and bond lengths are listed in Tables 2, S1 and S2,[†] respectively. Their CIF documents have also been deposited with Fachinformationszentrum Karlsruhe, 76344 Eggenstein-Leopoldshafen, Germany [fax: +49-7247-808-666; e-mail: crysdata@fiz.karlsruhe.de] with depository number CSD-432057 for 1, CSD-432055 for 2, CSD-432056 for 3 and CSD-432058 for 4.[†]

UV-Vis-NIR diffuse reflectance spectroscopies. The diffuse reflectance spectra were recorded at the room temperature on

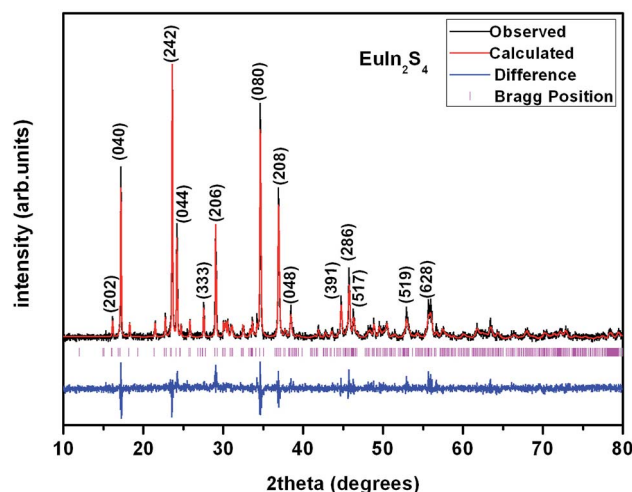


Fig. 1 Powder XRD pattern of 3. Calculated, experimental and residual diffraction patterns are marked with red, black and blue lines, respectively. Bragg reflections are indicated with vertical ticks. The relatively big residuals are caused by the orientation of the crystalline sample.



Table 2 Crystal data and structure refinement parameters of 1–4

Chemical formula	EuZnGeS ₄ (1)	EuGa ₂ S ₄ (2)	EuIn ₂ S ₄ (3)	EuIn ₂ Se ₄ (4)
F_w	418.16	419.64	509.84	697.44
T (K)	296			
Crystal system	Orthorhombic			
Space group	$Fddd$			
Z	32			
a (Å)	12.234(4)	12.209(11)	13.016(3)	13.490(1)
b (Å)	20.398(6)	20.445(18)	20.772(5)	21.748(1)
c (Å)	20.682(6)	20.680(19)	21.076(5)	21.859(1)
V (Å ³)	5161(3)	5162(8)	5699(2)	6412.9(6)
D_{calcd} (g cm ⁻³)	4.305	4.320	4.754	5.779
μ (mm ⁻¹)	19.076	19.048	16.166	31.487
$F(000)$	6048	6048	7200	9504
θ range (°)	2.18 to 25.50	2.18 to 25.49	2.08 to 25.48	2.01 to 27.50
Measd. reflns	5315	2843	9320	7650
Indep. reflns/ R_{int}	1203/0.0283	1171/0.0303	1329/0.0581	1844/0.0403
R_1/wR_2 ($I > 2\sigma(I)$) ^a	0.0483/0.1245	0.0342/0.0841	0.0327/0.0793	0.0287/0.0595
R_1/wR_2 (all data) ^a	0.0553/0.1279	0.0421/0.0894	0.0428/0.0878	0.0493/0.0666
GOF on F^2	1.129	1.145	1.090	1.093
$\Delta\rho_{\text{max}}/\Delta\rho_{\text{min}}$, e Å ⁻³	2.571/−1.815	3.368/−2.110	1.627/−2.332	2.042/−1.457

$$^a R_1 = \frac{\sum |F_o| - \sum |F_c|}{\sum |F_o|}; wR_2 = \frac{[\sum w(F_o^2 - F_c^2)^2]}{[\sum w(F_o^2)^2]}^{1/2}.$$

a computer-controlled Lambda 900 UV-Vis-NIR spectrometer equipped with an integrating sphere in the wavelength range of 200–1700 nm. A BaSO₄ plate was used as a reference, on which the finely ground powdery sample was coated. The absorption spectra were calculated from reflection spectrum by the Kubelka–Munk function.¹⁷

Calculation details. The calculation models were built directly from the single-crystal diffraction data of 1 and 2. The electronic structure calculation including band structure and density of states based on density functional theory (DFT) was performed using Material Studio.¹⁸ The generalized gradient approximation (GGA) was chosen as the exchange–correlation functional and a plane wave basis with the projector-augmented wave (PAW) potentials was used. The plane-wave cutoff energies of 1 and 2 are 480.0 eV and the threshold of 10⁻⁵ eV were set for the self-consistent-field convergence of the total electronic energy. The electronic configurations for Eu, Zn, Ge, Ga and S were 4f and 6s, 3d and 4s, 4s and 4p, 4s and 4p, and 3s and 3p, respectively. The numerical integration of the Brillouin zone was performed using 2 × 2 × 2 Monkhorst–Pack k -point meshes and the Fermi level ($E_f = 0$ eV) was selected as the reference.

Results and discussion

Crystal structure

Compounds 1–4 crystallize in the orthorhombic space group $Fddd$. The crystal structure of 1 is illustrated as a representative as they are isostructural. There are three Eu, one Zn, one Ge and four S atoms in the crystallographically independent unit. Its coordination geometry is shown in Fig. 2. All the three Eu atoms coordinated with eight neighboring S atoms to form EuS₈ bicapped trigonal prisms, Zn and Ge are fourfold-coordinated with four S atoms to form ZnS₄ or GeS₄ tetrahedron.

The structure can be viewed as layered if no consideration of the connection between Eu and S atoms (Fig. 3a). The layers

parallel to the ac plane are constructed by the connection between ZnS₄ and GeS₄ tetrahedra (Fig. 3b). It can be observed that either ZnS₄ or GeS₄ tetrahedra form dimers *via* sharing edges, respectively, namely, [Zn₂S₆]⁸⁻ or [Ge₂S₆]⁸⁻ units. Both of which are isolated and alternately linked to form the 2D structure. Take the whole structure consideration, the structure of 1 can be described as Eu–S bonds constructed 3D structure, and Zn²⁺ and Ge⁴⁺ cations occupy the tetrahedral cavities (Fig. 4a). It is necessary to understand how the EuS₈ bicapped trigonal prisms connect if we want to know how the 3D structure forms. The Eu atoms arrange regularly along the c direction. Eu(1) atoms arrange in a line along the c direction, while Eu(2) and Eu(3) atoms alternatively arrange in another line along the c direction. As shown in Fig. 4b, each EuS₈ units has six neighboring EuS₈ units, four of them connect with the central one *via* sharing edges, while the other two connected *via* sharing

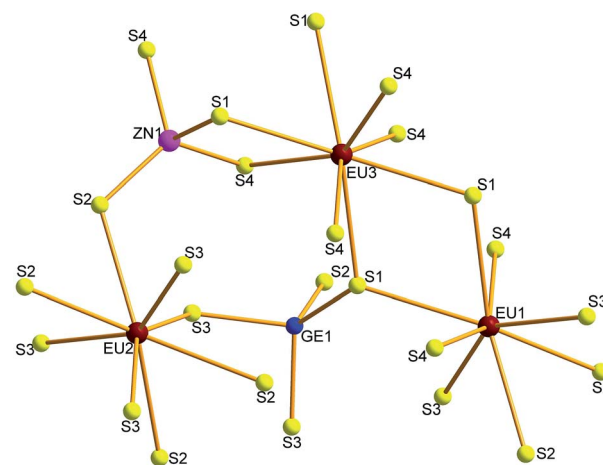


Fig. 2 Coordination geometry of 1.



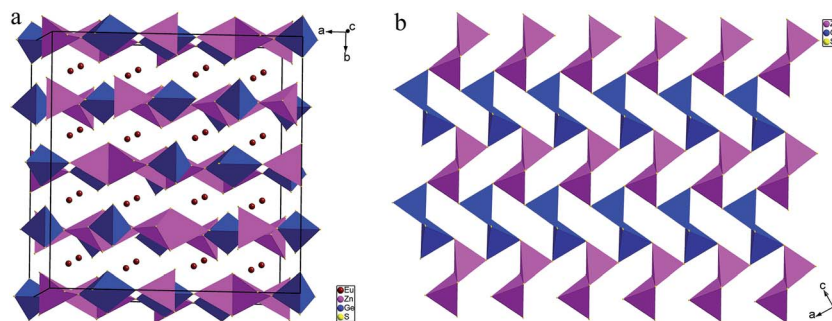


Fig. 3 (a) 2D structure of **1** constructed by the connection between GaS_4 and ZnS_4 tetrahedra. Eu–S bonds are omitted for clarity. (b) The $[\text{ZnGeS}_4]^{2-}$ layer viewed along the b direction. GaS_4 and ZnS_4 tetrahedra are represented as pink and blue polyhedra, respectively.

corners. The former and latter have the Eu–Eu distances of 5.208(2) and 5.947(1) Å, respectively.

The Zn–S and Ge–S bond lengths in **1** are in the range of 2.247(4)–2.303(5) and 2.246(4)–2.315(4) Å, respectively, which are in good agreement with 2.243(2)–2.305(2) Å of Ga–S bonds in **2**. These values are consistent with 2.242(1)–2.342(1) Å of Ga–S bonds in $(\text{K}_3\text{I})[\text{SmB}_{12}(\text{GaS}_4)_3]$.¹⁹ The Eu–S bonds in **1** have the distances of 3.070(4)–3.112(5) Å, similar with those discovered in RbEuGeS_4 .²⁰

As compounds **2–4** have more similar compositions. Here only the comparison is performed between **1** and **2**. There are two Ga sites in **2**, which can be substituted by one divalent and one tetravalent cations, respectively. So far, there are no quaternary II-III₂ (III-III')-Ch₄ or II-II'(I₂)-IV-Ch₄ compounds reported with $Fddd$ structure. Compound **1** represents the first one with this structure. It is interesting to study which one of the two Ga sites will be replaced by divalent cation. First, it has to be mentioned that both of the two Ga atoms occupy 32h sites. Second, both Zn and Ge positions are close to that of Ga in periodic table of the elements, so it is almost impossible to distinguish them by atomic weights when solving the structure.

Third, bond-valence calculation was performed on **2** to help determine which site will be occupied by Zn^{2+} ion, and the other one by Ge^{4+} ion. If Ga(1) and Ga(2) atoms are replaced by Zn and Ge atoms, respectively, their bond valences calculated to be 2.368 and 3.267, respectively. If Zn and Ge exchange their sites, their bond valences are 2.329 and 3.331, respectively. Even the calculation precision is considered, it is still difficult to determine that Ga(1) site is occupied by Zn or Ge atom. The most reasonable solution is that Zn and Ge atoms statistically co-occupy both of two Ga sites according to the bond-valence calculation results. For simplicity and convenience, the structure of **1** is described above as Zn and Ge atom completely occupy one Ga site, respectively. Definitely, the molar ratio of Zn and Ge should be 1 : 1 to maintain electric neutrality.

Optical properties

The UV-Vis-NIR diffuse reflectance spectra of **1–3** are shown in Fig. 5. Their optical band gaps are determined to be 2.26, 2.32 and 2.37 eV, respectively, which are consistent with their orange or yellow colors. Comparing these values, it may be proposed that there will be no big band gap change when the Ga atoms in

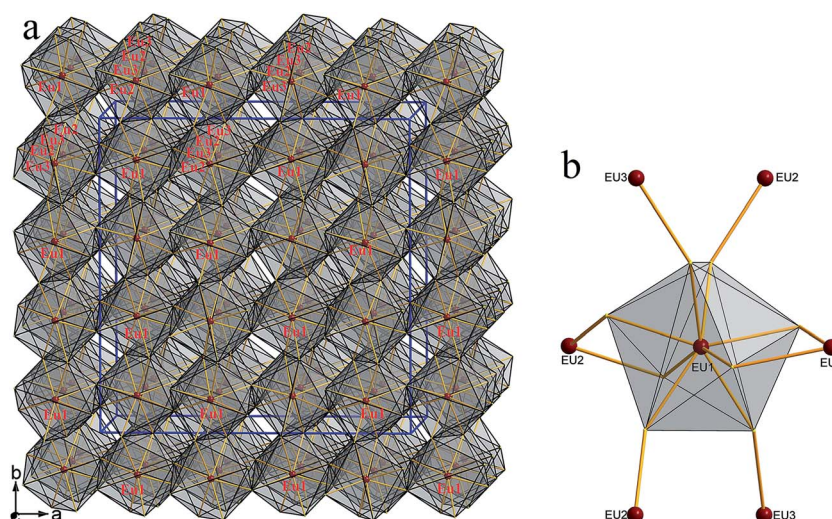


Fig. 4 (a) 3D framework constructed by the three types of EuS_8 bicapped trigonal prisms viewed along the c direction; (b) the neighboring Eu(2) and Eu(3) atoms around one Eu(1)S₈ unit.



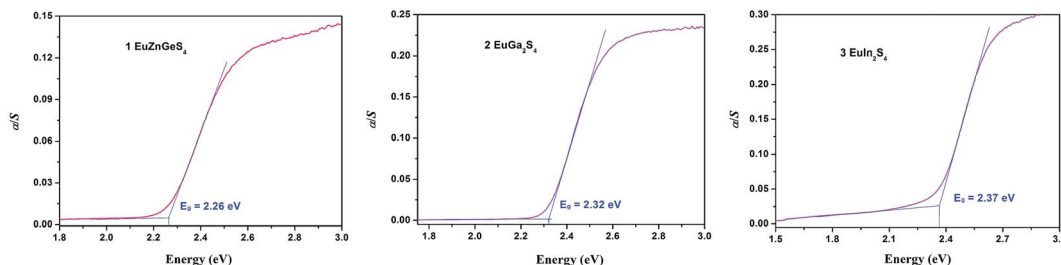


Fig. 5 Diffuse reflection spectra of 1–3.

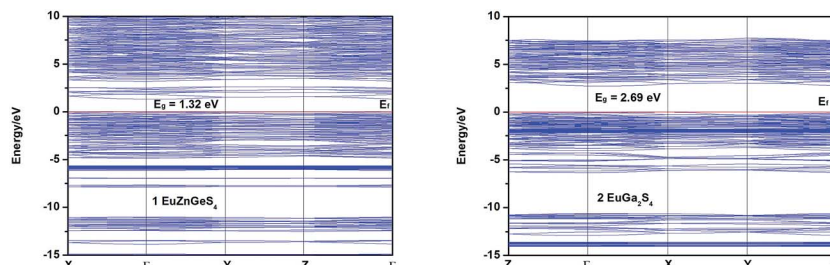


Fig. 6 Calculated band structures of 1 and 2. The Fermi level is chosen as the energy reference at 0 eV.

Table 3 Experimental and calculated optical band gaps of 1–3

		EuZnGeS ₄ (1)	EuGa ₂ S ₄ (2)	EuIn ₂ S ₄ (3)
Band gap (eV)	Experimental	2.26	2.32	2.37
	Calculated	1.32	2.69	—

EuGa₂S₄ are replaced by II + IV two types of atoms or by heavier III atoms like In atoms. This supposition may help design II-III₂ (III-III')-Ch₄ or II-II'(I₂)-IV-Ch₄ compounds with tunable band gaps.

Theory investigation

To investigate the electronic structures of 1 and 2, their band structures together with densities of states (DOS) computations based on the DFT theory were performed using Material Studio software.¹⁸ The calculated band structures along high symmetry points of the first Brillouin zone are shown in Fig. 6, from which

it can be seen that the band gaps of 1 and 2 are calculated to be 1.32 and 2.69 eV (Table 3), respectively, the former one is underestimated but reasonable in view of the calculation precision.²¹ Both the lowest conduction band (CB) and highest valence band (VB) of 1 are located at Γ point, indicating that 1 has a direct band gap. Different from 1, the CB and VB of 2 are located at Γ and X points, respectively, showing that 2 has an indirect band gap.

The total and partial densities of states (DOS and PDOS) of 1 and 2 are plotted in Fig. 7. For 1, the highest VB is mainly constituted of S-3p, and the lowest CB is mainly composed of Ge-4s and S-3p orbitals. The VBs between 0 and -5.0 eV are originated mainly from S-3p and Eu-4f orbitals. The CBs ranging from 2.5 to 7.5 eV are primarily consisted of Ge-4p, and minor Zn-4s and S-3p orbitals. Briefly, the band gap of 1 is determined by the S-3p and Ge-4s orbitals, the respective valence orbitals of S²⁻ and Ge⁴⁺ ions. For 2, the highest VB is mainly constituted of S-3p, and the lowest CB is mainly composed of Ga-4s, S-3p and Ga-4p orbitals, so its band gap is determined by valence orbitals of S²⁻ and Ga³⁺ ions. The VBs

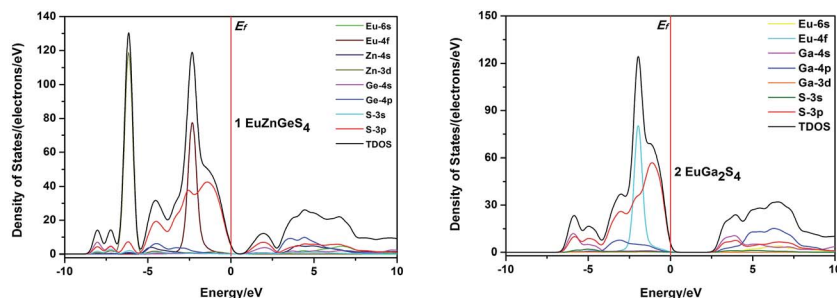


Fig. 7 Calculated density of states (DOS) of 1 and 2. The Fermi level is chosen as the energy reference at 0 eV.



from 0 to -4.0 eV are primarily consisted of S-3p, Eu-4f and minor Ga-4p orbitals. Comparing the PDOS of **1** and **2**, it can be concluded that the optical absorptions of **1** and **2** are mainly ascribed to the charge transitions from S-3p to valence orbitals of Ge^{4+} or Ga^{3+} cations.

It is well known that direct or indirect semiconductors have different applications in the optoelectronics research field. From EuGa_2S_4 to EuZnGeS_4 , two Ga^{3+} sites are replaced by one Zn^{2+} and one Ge^{4+} cations, which is a simple substitution but the parent structure EuGa_2S_4 can be maintained and the measured band gap have a little change. Together with the above discussion, it should be interesting to understand why semiconductor type can be changed while crystal structure and measured band gap keep stable. Besides, it seems the optical absorptions of **1** and **2** have little relationship with the valence orbitals of Eu^{2+} , which may give us some rules to explore II-III₂ (III-III')-Ch₄ or II-II'(I₂)-IV-Ch₄ compounds with desirable band gaps for their further photoelectric applications. One example might be used to verify this speculation. Other II-III₂-Ch₄ compounds containing divalent transition-metal, CdGa_2Se_4 and HgGa_2Se_4 , have direct band gaps of 2.40 and 1.93 eV, respectively, close to our sulfides.²² Besides, it is interesting to find that the calculated band gaps for compounds EuZnGeS_4 , CdGa_2Se_4 and HgGa_2Se_4 with direct band gaps are much lower than their experimental values.

Conclusions

Four isostructural europium chalcogenides were synthesized using solid-state reactions. Their measured band gaps indicate that they are semiconductors. Interestingly, the band gap type can be tuned from indirect to direct when using one divalent Zn^{2+} and one tetravalent Ge^{4+} cations to substitute the two trivalent Ga^{3+} cations sites in EuGa_2S_4 . This study may give some experience how to tune structures and band gaps of II-III₂ (III-III')-Ch₄ or quaternary II-II'(I₂)-IV-Ch₄ compounds (II = Mg, Ca, Sr, Ba, Eu and Yb; II' = divalent transition metal; I = Li, Na, Cu and Ag; III = B, Al, Ga and In; III' = Yb, Sb and Bi; IV = Ge and Sn; Ch = S, Se and Te).

Acknowledgements

We gratefully acknowledge financial support by the NSF of China (21673203), the Higher Education Science Foundation of Jiangsu Province (15KJB150031), State Key Laboratory of Structural Chemistry Fund (20150009), Natural Science Foundation of Yangzhou (YZ2016122) and the Priority Academic Program Development of Jiangsu Higher Education Institutions.

References

- (a) K. Mitchell and J. A. Ibers, *Chem. Rev.*, 2002, **102**, 1929–1952; (b) S.-P. Guo, G.-E. Wang, M.-J. Zhang, M.-F. Wu, G.-N. Liu, X.-M. Jiang, G.-C. Guo and J.-S. Huang, *Dalton Trans.*, 2013, **42**, 2679–2682; (c) Y. Chi, S.-P. Guo, H.-J. Kong and H.-G. Xue, *New J. Chem.*, 2016, **40**, 6720–6727.
- C.-Y. Meng, H. Chen, P. Wang and L. Chen, *Chem. Mater.*, 2011, **23**, 4910–4919.
- R. J. Yu, H. K. Yang, B. K. Moon, B. C. Choi and J. H. Jeong, *Phys. Status Solidi A*, 2012, **12**, 2620–2625.
- (a) H. J. Zhao, Y. F. Zhang and L. Chen, *J. Am. Chem. Soc.*, 2012, **134**, 1993–1995; (b) Y. F. Shi, Y. K. Chen, M. C. Chen, L. M. Wu, H. Lin, L. J. Zhou and L. Chen, *Chem. Mater.*, 2015, **27**, 1876–1884; (c) M. J. Zhang, B. X. Li, B. W. Liu, Y. H. Fan, X. G. Li, H. Y. Zeng and G. C. Guo, *Dalton Trans.*, 2013, **42**, 14223–14229.
- Z. Z. Luo, C. S. Lin, W. L. Zhang, H. Zhang, Z. Z. He and W. D. Cheng, *Chem. Mater.*, 2013, **26**, 1093–1099.
- Z. Z. Luo, C. S. Lin, W. D. Cheng, H. Zhang, W. L. Zhang and Z. Z. He, *Inorg. Chem.*, 2012, **52**, 273–279.
- K. Feng, X. Jiang, L. Kang, W. Yin, W. Hao, Z. S. Lin, J. Y. Yao, Y. C. Wu and C. T. Chen, *Dalton Trans.*, 2013, **42**, 13635–13641.
- C. Li, W. L. Yin, P. F. Gong, X. S. Li, M. L. Zhou, A. Mar, Z. S. Lin, J. Y. Yao, Y. C. Wu and C. T. Chen, *J. Am. Chem. Soc.*, 2016, **138**, 6135–6138.
- K. Wu, X. Su, S. L. Pan and Z. H. Yang, *Inorg. Chem.*, 2015, **54**, 2772–2779.
- K. Wu, X. Su, Z. H. Yang and S. L. Pan, *Dalton Trans.*, 2015, **44**, 19856–19864.
- (a) N. Zhen, K. Wu, Y. Wang, Q. Li, W. H. Gao, D. W. Hou, Z. H. Yang, H. D. Jiang, Y. J. Dong and S. L. Pan, *Dalton Trans.*, 2016, **45**, 10681–10688; (b) P. C. Donohue and J. E. Hanlon, *J. Electrochem. Soc.*, 1974, 137–142; (c) M. Tampier and D. Johrendt, *Z. Anorg. Allg. Chem.*, 2001, **627**, 312–320; (d) T. Sasaki, H. Takizawa, T. Takeda and T. Endo, *Mater. Res. Bull.*, 2003, **38**, 33–39; (e) T. Takizawa, C. Komatsu-Hidaka, K. Asaka, T. Isomoto and H. Matsushita, *Jpn. J. Appl. Phys.*, 2000, (Suppl. 39-1), 35–40; (f) A. Assoud, N. Soheilnia and H. Kleinke, *Chem. Mater.*, 2005, **17**, 2255–2261.
- (a) O. Gomis, R. Vilaplana, F. J. Manjón, E. Pérez-González, J. López-Solano, P. Rodríguez-Hernández, A. Muñoz, D. Errandonea, J. Ruiz-Fuertes, A. Segura, D. Santamaría-Pérez, I. M. Tiginyanu and V. V. Ursaki, *J. Appl. Phys.*, 2012, **111**, 013518; (b) O. Gomis, D. Santamaría-Pérez, R. Vilaplana, R. Luna, J. A. Sans, F. J. Manjón, D. Errandonea, E. Pérez-González, P. Rodríguez-Hernández, A. Muñoz and V. V. Ursaki, *J. Alloys Compd.*, 2014, **583**, 70–78; (c) O. Gomis, R. Vilaplana, F. J. Manjón, J. Ruiz-Fuertes, E. Pérez-González, J. López-Solano, E. Bandiello, D. Errandonea, A. Segura, P. Rodríguez-Hernández, A. Muñoz, V. V. Ursaki and I. M. Tiginyanu, *Phys. Status Solidi B*, 2015, **252**, 2043–2051; (d) J. Ruiz-Fuertes, D. Errandonea, F. J. Manjón, D. Martínez-García, A. Segura, V. V. Ursaki and I. M. Tiginyanu, *J. Appl. Phys.*, 2008, **103**, 063710; (e) O. Gomis, R. Vilaplana, F. J. Manjón, D. Santamaría-Pérez, D. Errandonea, E. Pérez-González, J. López-Solano, P. Rodríguez-Hernández, A. Muñoz, I. M. Tiginyanu and V. V. Ursaki, *J. Appl. Phys.*, 2013, **113**, 073510; (f) D. Errandonea, R. S. Kumar, F. J. Manjón, V. V. Ursaki and I. M. Tiginyanu, *J. Appl. Phys.*, 2008, **104**, 063524; (g) D. Errandonea, R. S. Kumar, O. Gomis,



- F. J. Manjón, V. V. Ursaki and I. M. Tiginyanu, *J. Appl. Phys.*, 2013, **114**, 233507; (h) D. Santamaría-Pérez, M. Amboage, F. J. Manjón, D. Errandonea, A. Muñoz, P. Rodríguez-Hernández, A. Mújica, S. Radescu, V. V. Ursaki and I. M. Tiginyanu, *J. Phys. Chem. C*, 2012, **116**, 14078–14087; (i) O. Gomis, R. Vilaplana, F. J. Manjón, D. Santamaría-Pérez, D. Errandonea, E. Pérez-González, J. López-Solano, P. Rodríguez-Hernández, A. Muñoz, I. M. Tiginyanu and V. V. Ursaki, *Mater. Res. Bull.*, 2013, **48**, 2128–2133.
- 13 (a) S.-P. Guo, Y. Chi and H.-G. Xue, *Inorg. Chem.*, 2015, **54**, 11052–11054; (b) Y. Chi and S.-P. Guo, *J. Mol. Struct.*, 2017, **1127**, 53–58; (c) Y. Chi, H.-J. Kong and S.-P. Guo, *Inorg. Chim. Acta*, 2016, **448**, 56–60; (d) S.-P. Guo, Y. Chi, B.-W. Liu and G.-C. Guo, *Dalton Trans.*, 2016, **45**, 10459–10465; (e) S.-P. Guo and G.-C. Guo, *J. Mater. Chem. A*, 2014, **2**, 20621–20628; (f) S.-P. Guo, Y. Chi, J.-P. Zou and H.-G. Xue, *New J. Chem.*, 2016, **40**, 10219–10226.
- 14 O. M. Aliev, *Inorg. Mater.*, 1980, **16**, 1027–1031.
- 15 (a) R. Roques, R. Rimet, J. P. Declercq and G. Germain, *Acta Crystallogr., Sect. B: Struct. Crystallogr. Cryst. Chem.*, 1979, **35**, 555–557; (b) T. E. Peters and J. A. Baglio, *J. Electrochem. Soc.*, 1972, **119**, 230–236.
- 16 Siemens, *SHELXTL™ Version 5 Reference Manual*, Siemens Energy & Automation Inc., Madison, Wisconsin, USA, 1994.
- 17 (a) W. W. Wendlandt and H. G. Hecht, *Reflectance Spectroscopy*, Interscience Publishers, New York, 1966; (b) G. Kortüm, *Reflectance Spectroscopy*, Springer, 1969.
- 18 M. D. Segall, P. J. D. Lindan, M. J. Probert, C. J. Pickard, P. J. Hasnip, S. J. Clark and M. C. Payne, *J. Phys.: Condens. Matter*, 2002, **14**, 2717–2744.
- 19 S. P. Guo, G. C. Guo, M. S. Wang, J. P. Zou, H. Y. Zeng, L. Z. Cai and J. S. Huang, *Chem. Commun.*, 2009, 4366–4368.
- 20 A. Choudhury, L. A. Polyakova, I. Hartenbach, T. Schleid and P. K. Dorhout, *Z. Anorg. Allg. Chem.*, 2006, **632**, 2395–2401.
- 21 (a) D. Errandonea, D. Martínez-García, R. Lacomba-Perales, J. Ruiz-Fuertes and A. Segura, *Appl. Phys. Lett.*, 2006, **89**, 091913; (b) R. Lacomba-Perales, D. Errandonea, A. Segura, P. Rodríguez-Hernández, S. Radescu, J. López-Solano, A. Mújica and A. Muñoz, *J. Appl. Phys.*, 2011, **110**, 043703; (c) V. Panchal, D. Errandonea, A. Segura, P. Rodríguez-Hernández, A. Muñoz, S. Lopez-Moreno and M. Bettinelli, *J. Appl. Phys.*, 2011, **110**, 043723.
- 22 F. J. Manjón, O. Gomis, P. Rodríguez-Hernández, E. Pérez-González, A. Muñoz, D. Errandonea, J. Ruiz-Fuertes, A. Segura, M. Fuentes-Cabrera, I. M. Tiginyanu and V. V. Ursaki, *Phys. Rev. B: Condens. Matter Mater. Phys.*, 2010, **81**, 195201.

